

Quantum Mechanical Exchange Coupling in Trihydridoosmium Complexes Containing Azole Ligands

Miguel A. Esteruelas,* Fernando J. Lahoz, Ana M. López, Enrique Oñate, Luis A. Oro, Natividad Ruiz, Eduardo Sola, and José I. Tolosa

Departamento de Química Inorgánica, Instituto de Ciencia de Materiales de Aragón, Universidad de Zaragoza-Consejo Superior de Investigaciones Científicas, 50009 Zaragoza, Spain

Received April 25, 1996[®]

The reaction of the hexahydrido complex $\text{OsH}_6(\text{P}^i\text{Pr}_3)_2$ (**1**) with 2,2'-biimidazole (H_2biim) leads to the trihydrido complex $\text{OsH}_3(\text{Hbiim})(\text{P}^i\text{Pr}_3)_2$ (**2**). Complex **2** reacts with the dimers $[\text{M}(\mu\text{-OME})(\text{COD})]_2$ ($\text{COD} = 1,5\text{-cyclooctadiene}$) to afford the heterobimetallic derivatives $(\text{P}^i\text{Pr}_3)_2\text{H}_3\text{Os}(\mu\text{-biim})\text{M}(\text{COD})$ ($\text{M} = \text{Rh}$ (**3**), Ir (**4**)). The structure of **4** was determined by an X-ray investigation. Complex **4** crystallizes in the triclinic space group $P\bar{1}$ (No. 2) with $a = 8.978(2)$ Å, $b = 13.629(3)$ Å, $c = 15.369(3)$ Å, $\alpha = 79.34(2)^\circ$, $\beta = 86.31(2)^\circ$, $\gamma = 72.43(1)^\circ$, and $Z = 2$. The coordination geometry around the osmium atom can be described as a distorted pentagonal bipyramid with the two phosphorus atoms of the phosphine ligands occupying *trans* positions. The osmium coordination sphere is completed by the hydrido ligands and by the chelating $\text{Ir}(\text{biim})(\text{COD})$ group, bonded through two nitrogen atoms. The H–H separations are 1.57(5) and 1.59(7) Å. Complex **1** also reacts with pyrazole (Hpz). The reaction gives $\text{OsH}_3(\text{pz})(\text{Hpz})(\text{P}^i\text{Pr}_3)_2$ (**5**), which affords $[\text{OsH}_3(\text{Hpz})_2(\text{P}^i\text{Pr}_3)_2]\text{BF}_4$ (**6**) and $\text{OsH}_3\text{Cl}(\text{Hpz})(\text{P}^i\text{Pr}_3)_2$ (**7**) by reaction with HBF_4 and HCl , respectively. The ^1H NMR spectra of **2–4** in the hydrido region at low temperature display AM_2X_2 spin systems ($\text{X} = ^{31}\text{P}$), which are simplified to AM_2 spin systems in the $^1\text{H}\{^{31}\text{P}\}$ spectra. The values for $J_{\text{A-M}}$ are abnormally large (between 31.7 and 76.0 Hz) and temperature dependent. Furthermore, they are inversely proportional to the electron density on the osmium atom, increasing in the sequence $2 < 3 < 4$. These results are interpreted in terms of the operation of quantum mechanical coupling between the hydrogen nuclei in the OsH_3 unit.

Introduction

The chemistry of transition-metal hydrido complexes is an area of great interest to organometallic chemists due to the possibilities offered by these compounds for the design of homogeneous catalysts¹ and the preparation of other types of complexes.² In the past few years, this chemistry has received increasing attention,³ while three major factors have contributed to the more recent development: (i) the discovery of transition-metal dihydrogen complexes by Kubas et al.⁴ (ii) the theoretical work by Burdett and co-workers suggesting that other polyhydrido ligands such as H_3 and H_4 may exist,⁵ and (iii) the observations of quantum mechanical exchange coupling between the hydrogen nuclei in some polyhydrido complexes.⁶

The quantum mechanical exchange coupling, which is presently attracting considerable interest, is revealed by abnormally

large and temperature dependent hydrogen–hydrogen coupling constants. Several trihydridos of $\text{Nb}^{6\text{h,i,j,m}}$, $\text{Mo}^{6\text{h}}$, $\text{Ru}^{6\text{d,f,g}}$ and $\text{Ir}^{6\text{c,e}}$ have been shown to display this behavior. For osmium, Heinekey and Harper have reported quantum mechanical exchange coupling between the hydrogen nuclei of the cationic complexes $[\text{OsH}_3(\eta^6\text{-C}_6\text{H}_6)(\text{PR}_3)]^+$ ($\text{PR}_3 = \text{PCy}_3$ ($\text{Cy} = \text{cyclohexyl}$), PPh_3 , $\text{MPTB} = 1\text{-methyl-4-phospha-3,6,8-trioxabicyclo-[2.2.2]octane}$),⁷ and Gusev and Caulton have observed the same phenomenon in the six-coordinate osmium (IV) derivatives $\text{OsH}_3\text{X}(\text{P}^i\text{Pr}_3)_2$ ($\text{X} = \text{Cl}, \text{Br}, \text{I}$) and in the trihydrido–dihydrogen $\text{OsH}_3(\eta^2\text{-H}_2)\text{I}(\text{P}^i\text{Pr}_3)_2$.⁸

[®] Abstract published in *Advance ACS Abstracts*, November 1, 1996.

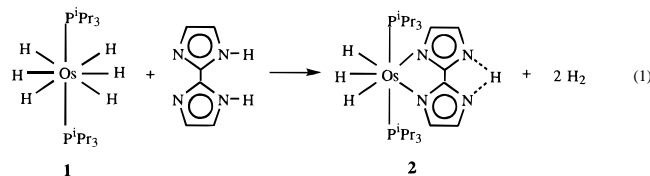
- (1) (a) James, B. R. *Homogeneous Hydrogenation*; John Wiley and Sons: New York, 1973. (b) Pignolet, L. H. *Homogeneous Catalysis with Metal Phosphine Complexes*; Plenum Press: New York, 1983. (c) Collman, J. P.; Heyedus, L. S. *Principles and Applications of Organotransition Metal Chemistry*; University Science Books: Mill Valley, CA, 1987. (d) Chaloner, P. A.; Esteruelas, M. A.; Joó, F.; Oro, L. A. *Homogeneous Hydrogenation*; Kluwer Academic Publishers: Dordrecht, The Netherlands, 1994.
- (2) Hlatky, G. G.; Crabtree, R. H. *Coord. Chem. Rev.* **1985**, *65*, 1.
- (3) (a) Kubas, G. J. *Comments Inorg. Chem.* **1987**, *7*, 17. (b) Kubas, G. J. *Acc. Chem. Res.* **1988**, *21*, 120. (c) Crabtree, R. H. *Acc. Chem. Res.* **1990**, *23*, 95. (d) Jessop, P. G.; Morris, R. H. *Coord. Chem. Rev.* **1992**, *121*, 155. (e) Crabtree, R. H. *Angew. Chem., Int. Ed. Engl.* **1993**, *32*, 789. (f) Heinekey, D. M.; Oldham, W. J. *Chem. Rev.* **1993**, *93*, 913.
- (4) Kubas, G. J.; Ryan, R. R.; Swanson, B. I.; Vergamini, P. J.; Wasserman, H. J. *J. Am. Chem. Soc.* **1984**, *106*, 451.
- (5) (a) Burdett, J. K.; Phillips, J. R.; Pourian, M. R.; Poliakov, M.; Turner, J. J.; Upmács, R. *Inorg. Chem.* **1987**, *26*, 3054. (b) Burdett, J. K.; Pourian, M. R. *Organometallics* **1987**, *6*, 1684.
- (6) (a) Heinekey, D. M.; Payne, N. G.; Schulte, G. K. *J. Am. Chem. Soc.* **1988**, *110*, 2303. (b) Antiñolo, A.; Chaudret, B.; Commenges, G.; Fajardo, M.; Jalon, F.; Morris, R. H.; Otero, A.; Schweltzer, C. T. *J. Chem. Soc., Chem. Commun.* **1988**, 1210. (c) Zilm, K. W.; Heinekey, D. M.; Millar, J. M.; Payne, N. G.; Demou, P. *J. Am. Chem. Soc.* **1989**, *111*, 3088. (d) Arliguie, T.; Border, C.; Chaudret, B.; Devillers, J.; Poilblanc, R. *Organometallics* **1989**, *8*, 1308. (e) Heinekey, D. M.; Millar, J. M.; Koetzle, T. F.; Payne, N. G.; Zilm, K. W. *J. Am. Chem. Soc.* **1990**, *112*, 909. (f) Heinekey, D. M.; Payne, N. G.; Sofield, C. D. *Organometallics* **1990**, *9*, 2643. (g) Arliguie, T.; Chaudret, B.; Jalon, F.; Otero, A.; López, J. A.; Lahoz, F. J. *Organometallics* **1991**, *10*, 1888. (h) Heinekey, D. M. *J. Am. Chem. Soc.* **1991**, *113*, 6074. (i) Barthelat, J. C.; Chaudret, B.; Daudey, J. P.; De Loth, Ph.; Poilblanc, R. *J. Am. Chem. Soc.* **1991**, *113*, 9896. (j) Antiñolo, A.; Carrillo, F.; Fernández-Baeza, J.; Otero, A.; Fajardo, M.; Chaudret, B. *Inorg. Chem.* **1992**, *31*, 5156. (k) Limbach, H. H.; Scherer, G.; Maurer, M.; Chaudret, B. *Angew. Chem., Int. Ed. Engl.* **1992**, *31*, 1369. (l) Jarid, A.; Moreno, M.; Lledós, A.; Lluch, J. M.; Bertrán, J. *J. Am. Chem. Soc.* **1993**, *115*, 5861. (m) Antiñolo, A.; Carrillo, F.; Chaudret, B.; Fajardo, M.; Fernández-Baeza, J.; Lanfranchi, M.; Limbach, H. H.; Maurer, M.; Otero, A.; Pellinghelli, M. A. *Inorg. Chem.* **1994**, *33*, 5163. (n) Jarid, A.; Moreno, M.; Lledós, A.; Lluch, J. M.; Bertrán, J. *J. Am. Chem. Soc.* **1995**, *117*, 1069. (o) Clot, E.; Leforestier, C.; Eisenstein, O.; Péliissier, M. *J. Am. Chem. Soc.* **1995**, *117*, 1797.
- (7) Heinekey, D. M.; Harper, T. G. P. *Organometallics* **1991**, *10*, 2891.
- (8) Gusev, D. G.; Kuhlman, R.; Sini, G.; Eisenstein, O.; Caulton, K. G. *J. Am. Chem. Soc.* **1994**, *116*, 2685.

For several years, we have studied the synthesis, reactivity, and catalytic potential of new dihydrogen and polyhydridoosmium compounds. Thus, 8 years ago, we reported the reaction of the five-coordinate complex $\text{OsHCl}(\text{CO})(\text{P}^i\text{Pr}_3)_2$ with NaBH_4 to afford $\text{OsH}(\eta^2\text{-H}_2\text{BH}_2)(\text{CO})(\text{P}^i\text{Pr}_3)_2$,⁹ which in the presence of 2-propanol decomposes to the tetrahydrido $\text{OsH}_4(\text{CO})(\text{P}^i\text{Pr}_3)_2$.¹⁰ This complex, which is an active catalyst for the hydrogen transfer from 2-propanol to ketones and α,β -unsaturated ketones,¹¹ reacts with terminal alkynes to give the alkynyl-hydrido-dihydrogen derivatives $\text{OsH}(\text{C}_2\text{R})(\eta^2\text{-H}_2)(\text{CO})(\text{P}^i\text{Pr}_3)_2$.¹² Similarly, the six-coordinate osmium(IV) complex $\text{OsH}_2\text{Cl}_2(\text{P}^i\text{Pr}_3)_2$ reacts with NaBH_4 to give $\text{OsH}_3(\eta^2\text{-H}_2\text{BH}_2)(\text{P}^i\text{Pr}_3)_2$,¹³ which, in the presence of 2-propanol, affords the hexahydrido $\text{OsH}_6(\text{P}^i\text{Pr}_3)_2$. This compound, which is also an active catalyst for the reduction of ketones by hydrogen transfer from 2-propanol,¹⁴ reacts with *N*-acetyl-L-cysteine to give the dihydrido $\text{OsH}_2\{\text{OC}(=\text{O})\text{CH}[\text{NHC}(=\text{O})\text{CH}_3]\text{CH}_2\text{S}\}(\text{P}^i\text{Pr}_3)_2$.¹⁵

As a continuation of our work in this field, we have now investigated the reactions of $\text{OsH}_6(\text{P}^i\text{Pr}_3)_2$ with 2,2'-biimidazole (H_2biim) and pyrazole (Hpz). During this study, we have observed that complex $\text{OsH}_3(\text{Hbiim})(\text{P}^i\text{Pr}_3)_2$ shows mechanical exchange coupling between the hydrogen nuclei of the OsH_3 unit, which can be increased by substitution of the acidic proton of the $[\text{Hbiim}]^-$ ligand by the metallic fragments $\text{M}(\text{COD})$ ($\text{M} = \text{Rh}, \text{Ir}$). In this paper, we report the synthesis and characterization of the first polyhydrido derivatives, containing nitrogen donor ligands, which show quantum mechanical exchange coupling.

Results and Discussion

2,2'-Biimidazole Compounds. Treatment of $\text{OsH}_6(\text{P}^i\text{Pr}_3)_2$ (**1**) with 2,2'-biimidazole in 1:1 molar ratio, in toluene under reflux, gives after 30 min a colorless solution from which the complex $\text{OsH}_3(\text{Hbiim})(\text{P}^i\text{Pr}_3)_2$ (**2**) is separated as a white solid in 85% yield, by addition of methanol. The formation of **2** can be rationalized in terms of the loss or four hydrogen atoms as molecular hydrogen, accompanied by the chelation of the monoanion $[\text{Hbiim}]^-$ to the central metal (eq 1). We suggest



that the first step of this reaction may be the protonation of **1** to give a cationic dihydrogen intermediate, probably $[\text{OsH}_3(\eta^2\text{-H}_2)(\text{P}^i\text{Pr}_3)_2]^+$, which rapidly reacts with $[\text{Hbiim}]^-$ by liberation of molecular hydrogen to afford **2**. In this context, it is noteworthy that a variety of polyhydridos of tungsten, rhenium, osmium, and iridium react with HBF_4 in acetonitrile to form

- (9) Werner, H.; Esteruelas, M. A.; Meyer, U.; Wrackmeyer, B. *Chem. Ber.* **1987**, *120*, 11.
 (10) Esteruelas, M. A.; Lahoz, F. J.; López, J. A.; Oro, L. A.; Schlünken, C.; Valero, C.; Werner, H. *Organometallics* **1992**, *11*, 2034.
 (11) (a) Esteruelas, M. A.; Sola, E.; Oro, L. A.; Werner, H.; Meyer, U. *J. Mol. Catal.* **1988**, *45*, 1. (b) Esteruelas, M. A.; Sola, E.; Oro, L. A.; Werner, H.; Meyer, U. *J. Mol. Catal.* **1989**, *53*, 43. (c) Esteruelas, M. A.; Valero, C.; Oro, L. A.; Meyer, U.; Werner, H. *Inorg. Chem.* **1991**, *30*, 1059.
 (12) Espuelas, J.; Esteruelas, M. A.; Lahoz, F. J.; Oro, L. A.; Valero, C. *Organometallics* **1993**, *12*, 663.
 (13) Esteruelas, M. A.; Jean, Y.; Lledós, A.; Oro, L. A.; Ruiz, N.; Volatron, F. *Inorg. Chem.* **1994**, *33*, 3609.
 (14) Aracama, M.; Esteruelas, M. A.; Lahoz, F. J.; López, J. A.; Meyer, U.; Oro, L. A.; Werner, H. *Inorg. Chem.* **1991**, *30*, 288.
 (15) Atencio, R.; Esteruelas, M. A.; Lahoz, F. J.; Oro, L. A.; Ruiz, N. *Inorg. Chem.* **1995**, *34*, 1004.

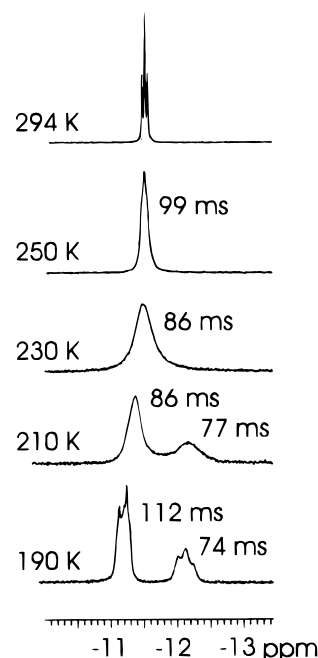


Figure 1. Variable temperature ^1H NMR spectra (300 MHz) in the high-field region of $\text{OsH}_3(\text{Hbiim})(\text{P}^i\text{Pr}_3)_2$ (**2**). T_1 for the intramolecular hydrogen exchange process are also provided.

molecular hydrogen and solvento complexes.¹⁶ Recently, Tilset and Caulton have also investigated the protonation of **1** with HBF_4 , which leads to the cationic dihydrogen complex $[\text{OsH}_3(\eta^2\text{-H}_2)(\text{P}^i\text{Pr}_3)_2]^+$. In acetonitrile, the nitrogen donor ligand displaces the two dihydrogen ligands to give $[\text{OsH}_3(\text{NCCH}_3)_2(\text{P}^i\text{Pr}_3)_2]^+$.¹⁷

The spectroscopic data of **2** are consistent with the formulation shown in eq 1. The IR spectrum in Nujol shows a very broad $\nu(\text{NH})$ absorption from 3000 to 2300 cm^{-1} , indicating the presence of a NH bond remaining in the coordinate monoanion $[\text{Hbiim}]^-$.¹⁸ In agreement with the mutually *trans* disposition of the phosphine ligands, at room temperature, the $^{31}\text{P}\{^1\text{H}\}$ NMR spectrum in toluene- d_8 shows a singlet at 19.8 ppm, which is temperature invariant down to 180 K. However, the ^1H NMR spectrum is temperature dependent. At room temperature, the spectrum exhibits in the hydrido region a single triplet resonance at -11.5 ppm with a P–H coupling constant of 12.90 Hz. This observation is consistent with the operation of a thermally activated site exchange process, which proceeds at a sufficient rate to lead to a single hydrido resonance. Consistent with this, lowering the sample temperature leads to broadening of the resonance. At very low temperature (210 K), decoalescence occurs and a pattern corresponding to an AM_2X_2 spin system ($\text{X} = ^{31}\text{P}$) is observed, which becomes well-resolved at 190 K (Figure 1). With ^{31}P decoupling (Figure 2a), the spectrum is simplified to the expected AM_2 spin system. Line shape analysis of the spectra of Figure 2a allows the calculation of the rate constants for the thermal exchange process at different temperatures. The activation parameters obtained from the Eyring analysis are $\Delta H^\ddagger = 9.29 \pm 0.22$ kcal mol^{-1} and $\Delta S^\ddagger = -2.85 \pm 0.67$ cal $\text{K}^{-1} \text{mol}^{-1}$. The value for the entropy of activation, close to zero, is in agreement with an intramolecular process, while the value for the enthalpy of

(16) Crabtree, R. H.; Hlatky, G. G.; Parnell, C. P.; Segmüller, B. E.; Uriarte, R. *J. Inorg. Chem.* **1984**, *23*, 354.

(17) Smith, K. T.; Tilset, M.; Kuhlman, R.; Caulton, K. G. *J. Am. Chem. Soc.* **1995**, *117*, 9473.

(18) (a) García, M. P.; López, A. M.; Esteruelas, M. A.; Lahoz, F. J.; Oro, L. A. *J. Chem. Soc., Dalton Trans.* **1990**, 3465. (b) Esteruelas, M. A.; Lahoz, F. J.; Oro, L. A.; Oñate, E.; Ruiz, N. *Inorg. Chem.* **1994**, *33*, 787.

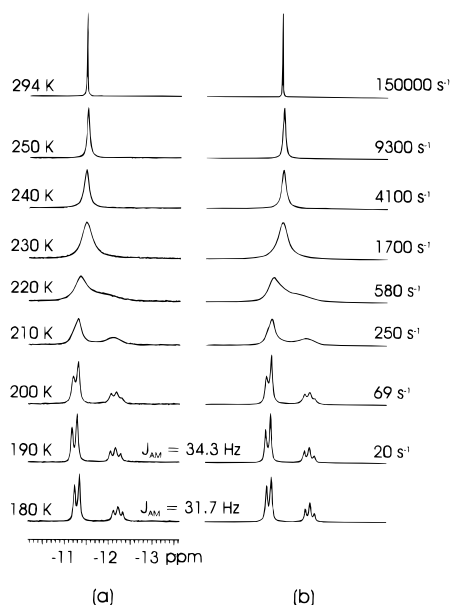


Figure 2. Observed $^1\text{H}\{^{31}\text{P}\}$ NMR spectra (300 MHz) (a) and simulated (b) in the high-field region of $\text{OsH}_3(\text{Hbiim})(\text{P}^i\text{Pr}_3)_2$ (**2**). Temperatures, rate constants for the intramolecular hydrogen site-exchange process, and H–H coupling constants are also provided.

activation lies in the range reported for similar thermal exchange processes in other trihydridos and hydrido–dihydrogen derivatives.¹⁹

The T_1 values of the hydrogen nuclei of the OsH_3 unit were determined over the temperature range of 190–250 K. At 230 K, the spectrum shows a broad resonance with a T_1 value of 86 ms. At 210 K, the spectrum contains two broad resonances as a result of the thermal exchange process between the protons M and A with a rate constant of 250 s^{-1} , and the T_1 values are 86 (M) and 77 ms (A). At 190 K, the T_1 values for the M and A signals are 112 and 74 ms, respectively (Figure 1).

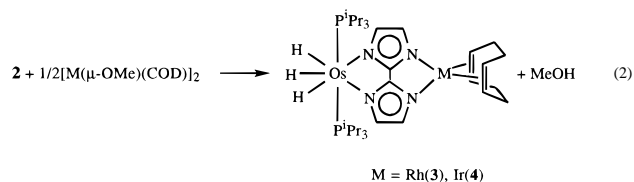
At very low temperatures the complexes of the general type $[\text{MH}(\eta^2\text{-H}_2)\text{L}_4]^+$ (M = Ru, Os) give rise to $^1\text{H}\{^{31}\text{P}\}$ NMR spectra which can be described as AM_2 spin systems for the hydrido region, with $J_{\text{A-M}}$ between 1 and 3 Hz. In this case, it has been previously proposed that above exchange rates of about 100 s^{-1} the observed relaxation rates are averages of the dihydrogen and hydrido rates, weighted 2:1.^{19a} Thus, we have calculated $1/T_1(\text{min})$ at 210 K for the hydrogen nuclei of the OsH_3 unit of **2** as the $1/T_1$ of the M and A signals weighted 2:1. The value obtained in this way is 12.1 s^{-1} . Since, the dipole–dipole interactions between the hydridos and between these ligands and the phosphine protons are responsible for the total relaxation rate, and the latter contribution has been estimated as $4\text{--}6\text{ s}^{-1}$ at 300 MHz,⁸ the remainder of the rate R ($6.1\text{--}8.1\text{ s}^{-1}$) leads to an estimated H–H distance of 1.71 \AA .²⁰

An AM_2 spin system is defined by the parameters δ_{A} , δ_{M} , and $J_{\text{A-M}}$. From the spectra at 190 and 180 K, values of -12.15 (δ_{A}), -11.25 (δ_{M}), and 34.3 (190 K) and 31.7 (180 K) ($J_{\text{A-M}}$) can readily be extracted and corroborated by computer simulation (Figure 2b). The complex $\text{OsH}_3(\eta^5\text{-C}_5\text{Me}_5)(\text{CO})$ ²¹ with a disposition for the hydrido ligands similar to that proposed for **2** displays $^1\text{H}\{^{31}\text{P}\}$ NMR spectra in the hydrido region which

can also be described as AM_2 spin systems. However, in these cases the value of $J_{\text{A-M}}$ is of the magnitude of 9 Hz. For **2** the large value of $J_{\text{A-M}}$ and its slight dependence on the temperature suggest the operation of quantum mechanical exchange coupling between the hydrogen nuclei in the OsH_3 unit.

In the iridium derivatives $[\text{IrH}_3(\eta^5\text{-C}_5\text{H}_5)(\text{PR}_3)]^+$ the exchange coupling decreases as the basicity of PR_3 increases.^{6c} The same trend has been observed for the cationic complexes $[\text{OsH}_3(\eta^6\text{-C}_6\text{H}_6)(\text{PR}_3)]^+$ which shows hydrogen–hydrogen coupling constants of 89 and 374 Hz, at 173 K, for R = Cy and Ph, respectively.⁷ Qualitatively, it has been proposed that the magnitude of the exchange coupling rapidly diminishes as the distances between the protons (a) is increased. The exchange coupling is also greatly diminished by decreasing the amplitude of the vibrational motion (δ).²² The large variations in the magnitude of the coupling are primarily due to an increase in δ with the less effective donor ligands.⁷ This implies that the lowering of the electron density at the metal center leads to increased motion of the hydrido ligands. In agreement with this Lledós has recently shown that the presence of a low-energy $\eta^2\text{-H}_2$ geometrical configuration makes hydrogen exchange possible through a tunneling exchange mechanism.⁶ⁿ As is well-known, good π -acceptor ligands tend to diminish the electronic density at the metallic center and, thus, the π -back-donation to the σ^* orbital of the molecular hydrogen.

Previously, we have reported that the complexes $\text{MH}(\text{Hbiim})(\text{CO})(\text{PPh}_3)_2$ (M = Ru, Os) react with the dimers $[\text{M}'(\mu\text{-OMe})(\text{COD})]_2$ (M' = Rh, Ir) to afford the corresponding heterobimetallic derivatives $[(\text{PPh}_3)_2(\text{CO})\text{HM}(\mu\text{-biim})\text{M}'(\text{COD})]$ and methanol. The replacement of the acidic proton of the $[\text{Hbiim}]^-$ ligand in $\text{MH}(\text{Hbiim})(\text{CO})(\text{PPh}_3)_2$ by $\text{M}'(\text{COD})$ units produces a significant decrease in the electron density of the M atoms, as shown by the shift of the $\nu(\text{CO})$ absorptions to higher frequencies. This reduction of electron density is higher for M' = Ir than for M' = Rh.^{18a} In order to decrease the energy of the $\eta^2\text{-H}_2$ transition state for the exchange coupling in this system, and, hence, to obtain complexes with larger hydrogen–hydrogen coupling constants than those observed for **2**, we have carried out the reactions of **2** with the dimers $[\text{M}'(\mu\text{-OMe})(\text{COD})]_2$. Treatment of **2** with these dimers in 2:1 molar ratio, in acetone under reflux, gives after 5 h yellow solutions from which the heterobimetallic derivatives **3** and **4** were obtained according to eq 2.



These complexes were isolated as yellow solids in 83% (**3**) and 81% (**4**) yield and characterized by IR and ^1H and $^{31}\text{P}\{^1\text{H}\}$ NMR spectroscopies. Complex **4** was further characterized by an X-ray crystallographic study. The molecular structure of **4** is presented in Figure 3. Selected bond distances and angles are listed in Table 1.

The biimidazole dianion coordinates as a planar ligand in a symmetrical tetradentate manner to the iridium and osmium. The coordination sphere around the iridium atom is approximately square-planar with the coordination polyhedron defined by two nitrogen atoms of the biimidazole and the midpoints of the two olefinic bonds of the cyclooctadiene ring. If M(1) and M(2) are the midpoints of the C(7)–C(8) and C(11)–C(12) bonds respectively, the deviations of M(1), M(2),

(19) (a) Earl, K. A.; Jia, G.; Maltby, P. A.; Morris, R. H. *J. Am. Chem. Soc.* **1991**, *113*, 3027. (b) Bautista, M. T.; Cappellani, E. P.; Drouin, S. D.; Morris, R. H.; Schweitzer, C. T.; Sella, A.; Zubkowski, J. J. *J. Am. Chem. Soc.* **1991**, *113*, 4876. (c) Jia, G.; Drouin, S. D.; Jessop, P. G.; Lough, A. J.; Morris, R. H. *Organometallics* **1993**, *12*, 906.

(20) The distance $r(\text{H-H})$ has been calculated from the following equation at 300 MHz: $R(\text{H-H}) = 129.18/[r(\text{H-H})]^6$, where $R(\text{H-H}) = 3R/4$ because of the C_{2v} geometry of the OsH_3 unit. See ref 8.

(21) Hoyano, J. K.; Graham, W. A. G. *J. Am. Chem. Soc.* **1982**, *104*, 3722.

(22) $J \cong -^3/4(3/\pi)^{1/2}h/2\pi m(a/\delta^3) \exp[-\{3(a^2 + \lambda^2)/4\delta^2\}]$. See ref 7.

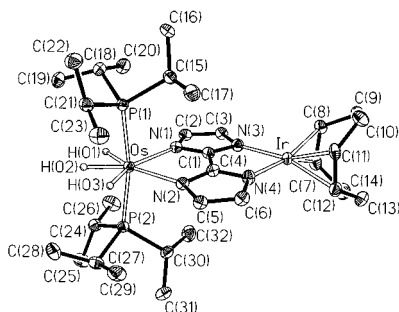


Figure 3. Molecular diagram of complex $(P^iPr_3)_2H_3Os(\mu\text{-biim})Ir(COD)$ (4). Thermal ellipsoids are shown at 50% probability.

Table 1. Selected Bond Lengths (Å) and Angles (deg) for the Complex $(P^iPr_3)_2H_3Os(\mu\text{-biim})Ir(COD)$ (4)

Os–P(1)	2.349(1)	N(2)–C(5)	1.402(5)
Os–P(2)	2.338(1)	N(4)–C(4)	1.329(5)
Os–N(1)	2.247(2)	N(4)–C(6)	1.379(4)
Os–N(2)	2.225(3)	C(5)–C(6)	1.379(5)
Os–H(01)	1.65(5)	H(01)···H(02)	1.57(5)
Os–H(02)	1.59(4)	H(02)···H(03)	1.59(7)
Os–H(03)	1.40(4)	Ir–N(3)	2.117(4)
N(1)–C(1)	1.312(5)	Ir–N(4)	2.116(3)
N(1)–C(2)	1.387(4)	Ir–C(7)	2.099(3)
N(3)–C(1)	1.336(4)	Ir–C(8)	2.118(3)
N(3)–C(3)	1.393(5)	Ir–C(11)	2.098(4)
C(2)–C(3)	1.387(5)	Ir–C(12)	2.112(4)
C(1)–C(4)	1.428(5)	C(7)–C(8)	1.421(6)
N(2)–C(4)	1.321(4)	C(11)–C(12)	1.424(5)
P(1)–Os–P(2)	168.53(3)	N(1)–Os–H(03)	158(2)
P(1)–Os–N(1)	92.91(8)	N(2)–Os–H(01)	157(2)
P(1)–Os–N(2)	93.71(8)	N(2)–Os–H(02)	145(1)
P(1)–Os–H(01)	91(2)	N(2)–Os–H(03)	81(2)
P(1)–Os–H(02)	86(1)	H(01)–Os–H(02)	58(2)
P(1)–Os–H(03)	91(2)	H(01)–Os–H(03)	122(3)
P(2)–Os–N(1)	97.83(8)	H(02)–Os–H(03)	64(2)
P(2)–Os–N(2)	92.51(8)	N(3)–Ir–N(4)	82.0(1)
P(2)–Os–H(01)	87(2)	N(3)–Ir–M(1) ^a	94.7(1)
P(2)–Os–H(02)	84(1)	N(3)–Ir–M(2) ^a	175.7(1)
P(2)–Os–H(03)	80(2)	N(4)–Ir–M(1) ^a	175.1(1)
N(1)–Os–N(2)	77.7(1)	N(4)–Ir–M(2) ^a	94.5(1)
N(1)–Os–H(01)	80(2)	M(1) ^a –Ir–M(2) ^a	88.9(2)
N(1)–Os–H(02)	137(1)		

^a M(1) and M(2) are the midpoints of the C(7)–C(8) and C(11)–C(12) olefin double bonds.

N(3), and N(4) from the mean plane passing through them are +0.076(4), –0.056(4), –0.034(3), and +0.050(3) Å, respectively, with the iridium atom deviating from this plane by –0.0001(2) Å. The Ir–N(3) and Ir–N(4) bond distances, 2.117(4) and 2.116(3) Å, are in the range found in related iridium biimidazole complexes.²³ The 1,5-cyclooctadiene ligand takes its customary “tub” conformation. The coordinated double bonds C(7)–C(8) and C(11)–C(12) have lengths of 1.421(6) and 1.424(5) Å, respectively, greater than in the free 1,5-cyclooctadiene molecule (1.34 Å),²⁴ in agreement with the usual Chatt–Dewar metal–olefin bonding scheme.

The coordination geometry around the osmium atom can be rationalized as a distorted pentagonal bipyramid with the two phosphorous atoms of the triisopropylphosphine ligands occupying *trans* positions (P(1)–Os–P(2) = 168.53(3)°). The osmium coordination sphere is completed by the hydride ligands, which were located in the final Fourier difference map, and by the chelate 2,2′-biimidazole ligand bonded through two nitrogen atoms.

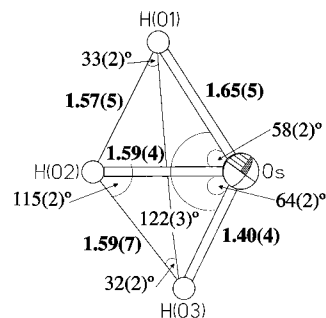


Figure 4. Geometry of the OsH_3 unit in $(P^iPr_3)_2H_3Os(\mu\text{-biim})Ir(COD)$ (4) from X-ray determination.

The hydride ligands and the osmium atom are strictly planar. The Os–H(01), Os–H(02), and Os–H(03) bond lengths are 1.65(5), 1.59(4), and 1.40(4) Å respectively, and the angles H(01)–Os–H(02), H(01)–Os–H(03) and H(02)–Os–H(03) are 58(2), 122(3), and 64(2)°, respectively. This disposition leads to a situation where the hydride ligands, between them, form the isosceles triangle shown in Figure 4.

The Os–N(1) (2.247(2) Å) and Os–N(2) (2.225(3) Å) distances are about 0.1 Å longer than the related bond lengths in cation $[OsCl(\eta^2\text{-H}_2)(H_2biim)(P^iPr_3)_2]^+$ (2.135(6) and 2.110(8) Å). However, the Os–P(1) (2.349(1) Å) and Os–P(2) (2.338(1) Å) distances are about 0.05 shorter than those found in the cationic derivative (2.396(2) and 2.390(2) Å).^{18b}

Each imidazole ring of the biimidazole ligand is strictly planar, but the ligand is slightly folded, making a dihedral angle of 8.0(1)°. Similar angles have been reported for the complexes $[(PPh_3)_2(CO)HRu(\mu\text{-biim})Rh(COD)]$ (2.6(2)°)^{18a} and $[Rh_4(CO)_8\text{-}(biim)_2]$ (4.0°),²⁵ whereas the two rings have been found to be coplanar in $[Rh(COD)]_2(\mu\text{-biim})$,²⁶ where the $[biim]^{2-}$ behaves as a symmetrical bichelating ligand as in 4.

The IR and ¹H and ³¹P{¹H} NMR spectra of 3 and 4 agree well with the structure shown in Figure 3. The IR spectra in Nujol contain $\nu(Os\text{-}H)$ absorptions at 2160 and 2130 (3) and 2175 and 2130 cm^{-1} (4). At room temperature, the ³¹P{¹H} NMR spectra in toluene-*d*₈ show singlets at 24.8 (3) and 25.7 ppm (4), which are temperature invariant down to 170 K. In accordance with the symmetrical square planar disposition of ligands around the rhodium and iridium atoms, for 3 and 4, respectively, the ¹H NMR spectra contain three resonances assignable to the diolefins: one due to the olefinic protons at about 4.3 ppm and the other two due to the aliphatic *exo* and *endo* protons at about 2.2 and 1.5 ppm. In the high-field region, the spectra are temperature dependent and similar to those shown in Figures 1 and 2. At room temperature, they exhibit a single triplet resonance at –12.35 (3) and –12.23 ppm (4) with P–H coupling constants of 12.5 and 12.4 Hz, respectively. Lowering the sample temperature leads to broadening of the resonances. At very low temperature (200 K for 3 and 190 K for 4), decoalescence occurs and patterns corresponding to AM_2X_2 spin systems are observed, which become well-resolved at 180 K. This behavior suggests that, in solution, for 2, there is an intramolecular exchange process involving the hydrogen atoms of the OsH_3 unit, which is thermally activated. Line shape analysis of the spectra allow the calculation of the rate constants for the thermal exchange processes at different temperatures. From the rate constants, the activation parameters collected in Table 2 were calculated by Eyring analysis.

The T_1 values for the hydrogen nuclei of the OsH_3 units of 3 and 4 were also determined over the temperature range of

(23) (a) Rasmussen, P. G.; Bailey, O. H.; Bayón, J. C.; Butler, W. M. *Inorg. Chem.* **1984**, *23*, 343. (b) Rasmussen, P. G.; Bailey, O. H.; Bayón, J. C. *Inorg. Chem.* **1984**, *23*, 338. (c) Rasmussen, P. G.; Anderson, J. E.; Bailey, O. H.; Tamres, M.; Bayón, J. C. *J. Am. Chem. Soc.* **1985**, *107*, 279.

(24) Churchill, M. R.; Bezman, S. A. *Inorg. Chem.* **1973**, *12*, 531.

(25) Kaiser, S. W.; Saillant, R. B.; Butler, W. M.; Rasmussen, P. G. *Inorg. Chem.* **1976**, *15*, 2688.

(26) Kaiser, S. W.; Saillant, R. B.; Butler, W. M.; Rasmussen, P. G. *Inorg. Chem.* **1976**, *15*, 2681.

Table 2. Activation Parameters for the Intramolecular Exchange Process Involving the Hydrido Ligands of **2–4**, H–H Coupling Constants between These Ligands, and $\Delta\nu(\text{CO})$ for Complexes Related to **2–4**

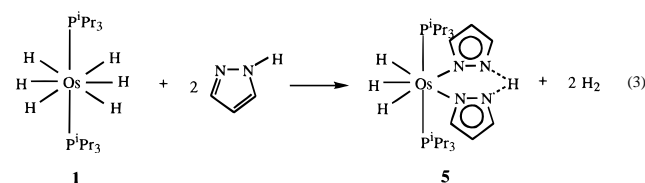
complex	ΔH^a	ΔS^b	$J_{\text{H-H}}^c$	$\Delta\nu(\text{CO})^{d,e}$
2	9.29 ± 0.22	-2.85 ± 0.67	34.3 (190 K)	5 (Ru–Rh)
			31.7 (180 K)	
3	8.05 ± 0.18	-4.69 ± 0.62	52.3 (180 K)	15 (Ru–Ir)
			50.3 (170 K)	
4	7.19 ± 0.16	-7.15 ± 0.55	76.0 (180 K)	10 (Os–Ir)
			68.6 (170 K)	

^a Unit: kcal mol⁻¹. ^b Unit: cal K⁻¹ mol⁻¹. ^c Unit: Hz. ^d $\Delta\nu(\text{CO}) = \nu(\text{CO})[(\text{PPh}_3)_2(\text{CO})\text{HM}(\mu\text{-biim})\text{M}(\text{COD})] - \nu(\text{CO})[\text{MH}(\text{Hbiim})(\text{CO})(\text{PPh}_3)_2]$. ^e Unit: cm⁻¹.

190–290 K. For **3**, a $T_1(\text{min})$ value of 81 ms was obtained at 230 K, at which point, the spectrum shows a broad resonance as a result of the thermal exchange process occurring at 9900 s⁻¹. This $T_1(\text{min})$ value permits an estimate of the H–H distance of 1.70 Å.²⁰ For **4**, the $T_1(\text{min})$ was also obtained at 230 K, when the thermal exchange process occurs at 20 500 s⁻¹, and the spectrum shows a broad resonance. Its value (76 ms) corresponds to a H–H distance of 1.67 Å.²⁰

As expected, the reduction of electron density on the osmium atom produces an increase in the hydrogen–hydrogen coupling constants of the hydrogen nuclei of the OsH₃ unit. At 180 K this increase is of 20.6 Hz in going from **2** to **3** and 23.7 Hz from **3** to **4** (Table 2). The data collected in Table 2 deserve further comment. Although the values of activation parameters must be considered with care due to the quantum mechanical exchange coupling, they show a definite trend that cannot be overlooked. Thus, the values of ΔS^\ddagger are slightly negative, becoming more negative as the electron density on the osmium atom is reduced. This is in full agreement with the presence of a thermally accessible $\eta^2\text{-H}_2$ transition state. Furthermore, the reduction of electron density on the osmium atom leads to a decrease in the enthalpy of activation of the exchange process, which permits an increase in the value of the hydrogen–hydrogen coupling constants. In this context, it should be noted that theoretical studies on the quantum mechanical hydrogen exchange coupling in $[\text{IrH}_3(\eta^5\text{-C}_5\text{H}_5)\text{L}]^+$ suggest that an increase in the energy barrier of the exchange process involves a decrease in the hydrogen–hydrogen coupling constant.⁶ⁿ

Pyrazole Compounds. Treatment of **1** with pyrazole in 1:2 molar ratio, during 45 min in toluene under reflux, produces gas evolution and formation of a colorless solution from which the complex OsH₃(pz)(Hpz)(PⁱPr₃)₂ (**5**) is separated as a white solid in 85% yield, by addition of methanol (eq 3). The reaction, most probably, proceeds by a mechanism similar to that proposed for the formation of **2**. One pyrazole protonates the starting complex to give $[\text{OsH}_3(\eta^2\text{-H}_2)_2(\text{P}^i\text{Pr}_3)_2]^+$, and the resulting pyrazolato anion and the other pyrazole substitute the dihydrogen ligands.



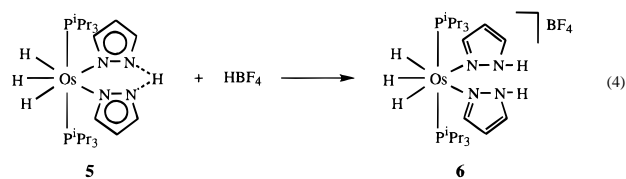
The ¹H NMR spectrum of **5** in benzene-*d*₆ contains four broad singlets at 21.4 (NHN), 7.96 (NCH), 7.60 (NCH), and 6.32 (CH) ppm. The relative intensity of the peaks is respectively 1:2:2:2. The ¹H NMR spectrum also contains, along with the triisopropylphosphine resonances, a high-field triplet at -11.92 ppm with a P–H coupling constant of 12.5 Hz. The ³¹P{¹H} NMR spectrum shows a singlet at 22.8 ppm, which splits into

a quartet when only the protons of the triisopropyl groups are irradiated. This is in agreement with the presence of three hydrogen atoms directly linked to an osmium center containing two equivalent phosphine ligands *trans* disposed.

The ³¹P{¹H} NMR spectrum is temperature invariant. However, in the ¹H NMR spectrum the signal of the hydrido ligands undergoes broadening at temperatures lower than room temperature. This signal gives a minimum for the relaxation time T_1 of 74 ms at 213 K, suggesting a separation between the hydrido ligands of about 1.66 Å.

We note that the related ruthenium derivative has been recently reported.²⁷ In contrast to **5**, it is a hydrido–dihydrogen derivative. This agrees well with the known qualitative difference between phosphine polyhydrido complexes of osmium and ruthenium. While the former are typically classical (e.g. OsH₆(PR₃)₂,^{14,28} OsH₄(PR₃)₃,²⁹ OsH₄(CO)(PR₃)₂,⁹ and OsH₃X(PR₃)₂⁸), the latter generally contain at least one dihydrogen ligand (RuH₂($\eta^2\text{-H}_2$)₂(PR₃)₂,³⁰ RuH₂($\eta^2\text{-H}_2$)(PR₃)₃,^{29b} RuH₂($\eta^2\text{-H}_2$)(CO)(PR₃)₂,³¹ and RuH($\eta^2\text{-H}_2$)X(PR₃)₂³²).

Complex **5** does not react with $[\text{M}(\mu\text{-OMe})(\text{COD})]_2$ (M = Rh, Ir). However, the addition of the stoichiometric amount of HBF₄·OEt₂ to **5** in diethyl ether precipitates a white solid, analyzed as $[\text{OsH}_3(\text{Hpz})_2(\text{P}^i\text{Pr}_3)_2]\text{BF}_4$ (**6**) (eq 4). The yield of this reaction is 90%.



The IR spectrum of **6** in Nujol contains a strong and broad $\nu(\text{NH})$ absorption centered at 3350 cm⁻¹, a $\nu(\text{Os-H})$ band at 2160 cm⁻¹, and the absorption due to $[\text{BF}_4]^-$ with T_d symmetry between 1200 and 980 cm⁻¹. At room temperature, the ¹H NMR spectrum contains a triplet at -12.53 ppm with a P–H coupling constant of 12.4 Hz, the phosphine resonances, and four broad singlets of the same intensity at 10.72, 7.85, 7.80, and 6.45 ppm assigned to the pyrazole protons. The ³¹P{¹H} NMR spectrum shows a singlet at 24.5 ppm, which under off-resonance conditions is split into a quartet due to the P–H coupling.

Complex **6** is very similar to the acetonitrile derivative $[\text{OsH}_3(\text{NCCH}_3)_2(\text{P}^i\text{Pr}_3)_2]\text{BF}_4$, recently reported by Tilset and Caulton,¹⁷ and in the hydrido region of the ¹H NMR spectrum both compounds show the same behavior. Below room temperature, the hydrido resonances undergo broadening but show no sign of decoalescence. The $T_1(\text{min})$ value of the hydrido resonance of **6** is 67 ms at 213 K, which permits an estimate of the H–H distance of about 1.61 Å.²⁰ For the acetonitrile derivative a H–H separation of 1.57 Å has been proposed.¹⁷

When **6** is stirred with the stoichiometric amount of NaCl for 30 min in THF at room temperature, a further reaction occurs (eq 5) to give OsH₃Cl(Hpz)(PⁱPr₃)₂ (**7**) as a white solid in 44% yield. A more direct route to **7**, avoiding the isolation of **6**, involves the addition of a stoichiometric amount of a HCl–

(27) Christ, M. L.; Sabo-Etienne, S.; Chung, G.; Chaudret, B. *Inorg. Chem.* **1994**, *33*, 5316.

(28) Howard, J. A. K.; Johnson, O.; Koetzle, T. F.; Spencer, J. L. *Inorg. Chem.* **1987**, *26*, 2930.

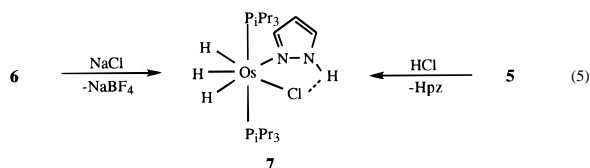
(29) (a) Hart, D. W.; Bau, R.; Koetzle, T. F. *J. Am. Chem. Soc.* **1977**, *99*, 7557. (b) Crabtree, R. H.; Hamilton, D. G. *J. Am. Chem. Soc.* **1986**, *108*, 3124.

(30) Chaudret, B.; Poilblanc, R. *Organometallics* **1985**, *4*, 1722.

(31) Gusev, D. G.; Vymenits, A. B.; Bakmutov, V. I. *Inorg. Chem.* **1992**, *31*, 2.

(32) Chaudret, B.; Chung, G.; Eisenstein, O.; Jackson, S. A.; Lahoz, F. J.; López, J. A. *J. Am. Chem. Soc.* **1991**, *113*, 2314.

toluene solution to **5** in toluene. By this procedure **7** was obtained in 40%.



The IR and NMR spectra of **7** are in good agreement with the proposed structure. The IR spectrum in Nujol shows two $\nu(\text{Os}-\text{H})$ bands at 2148 and 2172 cm^{-1} , as well as a strong and lightly broad band at 3228 cm^{-1} for $\nu(\text{N}-\text{H})$ coordinated pyrazole. The lower wavenumber compared with that of **6** can be attributed to the presence of a hydrogen bond $\text{N}-\text{H}\cdots\text{Cl}$.^{33,34} At room temperature, the ^1H NMR spectrum contains four broad signals at 13.35, 7.50, 6.37, and 5.73 ppm, due to the hydrogen of the pyrazole, along with the phosphine resonances and a triplet at -12.83 ppm with a P–H coupling constant of 12.6 Hz. This spectrum is also temperature dependent. Lowering the sample temperature leads to broadening of the triplet. At 193 K, a first decoalescence into two broad peaks at -12.2 and -13.7 ppm is observed, and at 178 K decoalescence of the signal at low field occurs. A $T_1(\text{min})$ value of 71 ms was obtained at 213 K. This value supports the hydrido character of **7** and suggests that the separation between the hydrido ligands is similar to those calculated for the other trihydrido–azole compounds. At room temperature the $^{31}\text{P}\{^1\text{H}\}$ NMR spectrum shows a singlet at 23.7 ppm, which under off-resonance conditions is split into the expected quartet due to the P–H coupling.

Concluding Remarks

This study has shown that the hexahydrido $\text{OsH}_6(\text{P}^i\text{Pr}_3)_2$ reacts with 2,2'-biimidazole and pyrazole to give the trihydrido derivatives $\text{OsH}_3(\text{Hbiim})(\text{P}^i\text{Pr}_3)_2$ and $\text{OsH}_3(\text{pz})(\text{Hpz})(\text{P}^i\text{Pr}_3)_2$. The reactions of $\text{OsH}_3(\text{Hbiim})(\text{P}^i\text{Pr}_3)_2$ with the dimers $[\text{M}(\mu\text{-OMe})(\text{COD})]_2$ ($\text{M} = \text{Rh}, \text{Ir}$) afford the heterobimetallic complexes $(\text{P}^i\text{Pr}_3)_2\text{H}_3\text{Os}(\mu\text{-biim})\text{M}(\text{COD})$ ($\text{M} = \text{Rh}, \text{Ir}$). The complex $\text{OsH}_3(\text{pz})(\text{Hpz})(\text{P}^i\text{Pr}_3)_2$ does not react with the dimers $[\text{M}(\mu\text{-OMe})(\text{COD})]_2$ ($\text{M} = \text{Rh}, \text{Ir}$). However, it leads to $[\text{OsH}_3(\text{Hpz})_2(\text{P}^i\text{Pr}_3)_2]\text{BF}_4$ and $\text{OsH}_3\text{Cl}(\text{Hpz})(\text{P}^i\text{Pr}_3)_2$ by reaction with HBF_4 and HCl , respectively. The coordination geometry around the osmium atom of these compounds can be described as a distorted pentagonal bipyramid, where the hydrido ligands, which are coplanar with the osmium atom, are separated by distances between 1.71 and 1.61 Å.

The biimidazole compounds are the first polyhydrido derivatives, containing nitrogen donor ligands, which show mechanical exchange coupling between the hydrogen nuclei of the OsH_3 unit. The heterobimetallic complexes give rise to H–H coupling constants larger than those of the mononuclear derivative, and the H–H coupling constants in the heterobimetallic Os–Ir compound are also larger than those of the heterobimetallic Os–Rh. The origin of this increase can be explained in terms of electron density reduction on the osmium atom, which is a result of the replacement of the acidic proton of the $[\text{Hbiim}]^-$ ligand in the mononuclear complex by the $\text{M}(\text{COD})$ units.

Previously, we have reported that the coordination of a metallic fragment to a homogeneous catalyst in nonactive sites produces an enhancement of the activity on the system. This effect has electronic origin, a result of electronic communication

between the metal centers through the bridging ligands.³⁵ Here, we show that the same type of synergism can be applied to the quantum mechanical exchange coupling.

Experimental Section

Physical Measurements. Infrared spectra were recorded as Nujol mulls on polyethylene sheets using a Perkin-Elmer 883 or a Nicolet 550 spectrometer. NMR spectra were recorded on a Varian XL 200 or UNITY 300 or on a Bruker ARX 300. The probe temperature of the NMR spectrometers was calibrated against a methanol standard. ^1H chemical shifts were measured relative to partially deuterated solvent peaks but are reported relative to tetramethylsilane. $^{31}\text{P}\{^1\text{H}\}$ chemical shifts are reported relative to H_3PO_4 (85%). Coupling constants J and N ($N = J(\text{HP}) + J(\text{HP}')$) are given in hertz. C, H analyses were carried out in a Perkin-Elmer 2400 CHNS/O analyzer.

Kinetic Analysis. Complete line shape analysis of the $^1\text{H}\{^{31}\text{P}\}$ NMR spectra was achieved by using the program DNMR6 (QCPE, Indiana University). The rate constants for various temperatures were obtained by visually matching observed and calculated spectra. The transverse relaxation times T_2 used were obtained from spectra for all temperatures recorded, from the line width of the biimidazole ligand proton resonances. The activation parameters ΔH^\ddagger and ΔS^\ddagger were calculated by least-squares fit of $\ln(k/T)$ vs $1/T$ (Eyring equation). Error analysis assumed a 10% error in the rate constant and 1 K in the temperature. Errors were computed by published methods.³⁶

Synthesis. All reactions were carried out with exclusion of air using standard Schlenk techniques. Solvents were dried by known procedures and distilled under argon prior to use. The complexes $\text{OsH}_2\text{Cl}_2(\text{P}^i\text{Pr}_3)_2$ and $\text{OsH}_6(\text{P}^i\text{Pr}_3)_2$ (**1**) were prepared according with the literature method.¹⁴

Preparation of $\text{OsH}_3(\text{Hbiim})(\text{P}^i\text{Pr}_3)_2$ (2**).** A suspension of $\text{OsH}_2\text{Cl}_2(\text{P}^i\text{Pr}_3)_2$ (200 mg, 0.35 mmol) in 16 mL of toluene was first treated with NaBH_4 (133 mg, 3.5 mmol) and then dropwise with 1.8 mL of methanol. After being stirred for 15 min at room temperature, the solution was filtered through Kieselguhr. The filtrate was treated with 2,2'-biimidazole (H_2biim) (47 mg, 0.35 mmol) and heated under reflux for 30 min. The colorless solution was filtered through Kieselguhr and concentrated to ca. 0.5 mL. Addition of methanol caused the precipitation of a white solid. The solvent was decanted, and the solid washed twice with methanol and dried in vacuo: yield 192 mg (85%). IR (Nujol): $\nu(\text{NH})$ 2300–3000, $\nu(\text{OsH})$ 2120 cm^{-1} . ^1H NMR (300 MHz, CD_2Cl_2 , 293 K): δ 7.13 and 7.07 (both br, each 2 H, =CH biim), 1.61 (m, 6 H, PCH), 0.91 (dvt, $N = 12.4$ Hz, $J(\text{HH}) = 6.7$ Hz, 36 H, PCCH_3), -11.53 (t, $J(\text{PH}) = 12.9$ Hz, 3 H, OsH). $^{31}\text{P}\{^1\text{H}\}$ NMR (80.98 MHz, C_6D_6): δ 19.80 (s). Anal. Calcd for $\text{C}_{24}\text{H}_{50}\text{N}_4\text{OsP}_2$: C, 44.56; H, 7.81; N, 8.65. Found: C, 44.07; H, 8.22; N, 8.40. T_1 (ms, OsH_3 , 300 MHz, CD_2Cl_2): 99 (250 K); 86 (230 K); 86, 77 (210 K); 112, 74 (190 K).

Preparation of $(\text{P}^i\text{Pr}_3)_2\text{H}_3\text{Os}(\mu\text{-biim})\text{Rh}(\text{COD})$ (3**).** A suspension of **2** (100 mg, 0.15 mmol) in 15 mL of acetone was treated with $[\text{Rh}(\mu\text{-OMe})(\text{COD})]_2$ (37 mg, 0.075 mmol). The sample was stirred and heated under reflux for 5 h. The yellow solution was filtered through Kieselguhr and concentrated to ca. 0.1 mL. Addition of methanol caused the precipitation of a yellow solid, which was decanted, washed twice with methanol, and dried in vacuo: yield 107 mg (83%). IR (Nujol): $\nu(\text{OsH})$ 2160, 2130 cm^{-1} . ^1H NMR (300 MHz, C_6D_6 , 293 K): δ 7.15 and 6.64 (both br, each 2 H, =CH biim), 4.40 (br, 4 H, =CH COD), 2.19 (br, 4 H, CH_2 COD), 1.73 (m, 6 H, PCH), 1.53 (m, 4 H, CH_2 COD), 1.01 (dvt, $N = 12.6$ Hz, $J(\text{HH}) = 6.6$ Hz, 36 H, PCCH_3), -12.35 (t, $J(\text{PH}) = 12.5$ Hz, 3 H, OsH). $^{31}\text{P}\{^1\text{H}\}$ NMR (80.98 MHz, C_6D_6): δ 24.80 (s). Anal. Calcd for $\text{C}_{32}\text{H}_{61}\text{N}_4\text{OsP}_2\text{Rh}$: C, 44.84; H, 7.19; N, 6.54. Found: C, 44.47; H, 7.43; N, 6.62. T_1 (ms, OsH_3 , 300 MHz, toluene- d_8): = 177 (290 K), 88 (250 K), 81 (230 K), 123 (210 K).

Preparation of $(\text{P}^i\text{Pr}_3)_2\text{H}_3\text{Os}(\mu\text{-biim})\text{Ir}(\text{COD})$ (4**).** The complex was prepared analogously to that described for **3**, starting from **2** (100

(33) García, M. P.; Esteruelas, M. A.; Martín, M.; Oro, L. A. *J. Organomet. Chem.* **1994**, *467*, 151.

(34) Atencio, R.; Bohanna, C.; Esteruelas, M. A.; Lahoz, F. J.; Oro, L. A. *J. Chem. Soc., Dalton Trans.* **1995**, 2171.

(35) (a) García, M. P.; López, A. M.; Esteruelas, M. A.; Lahoz, F. J.; Oro, L. A. *J. Chem. Soc., Chem Commun.* **1988**, 793. (b) Esteruelas, M. A.; García, M. P.; López, A. M.; Oro, L. A. *Organometallics* **1991**, *10*, 127. (c) Esteruelas, M. A.; García, M. P.; López, A. M.; Oro, L. A. *Organometallics* **1992**, *11*, 702.

(36) Morse, P. M.; Spencer, M. O.; Wilson, S. R.; Girolami, G. S. *Organometallics* **1994**, *13*, 1646.

mg, 0.15 mmol) and [Ir(μ -OMe)(COD)]₂ (51 mg, 0.075 mmol). A yellow solid was obtained: yield 115 mg (81%). IR (Nujol): ν (OsH) 2175, 2130 cm⁻¹. ¹H NMR (300 MHz, C₆D₆, 293 K): δ 7.06 and 6.71 (both br, each 2 H, =CH biim), 4.25 (br, 4 H, =CH COD), 2.16 (br, 4 H, CH₂ COD), 1.70 (m, 6 H, PCH), 1.43 (m, 4 H, CH₂ COD), 0.97 (dvt, $N = 12.4$ Hz, $J(\text{HH}) = 6.9$ Hz, 36 H, PCCH₃), -12.23 (t, $J(\text{PH}) = 12.4$ Hz, 3 H, OsH). ³¹P{¹H} NMR (121.42 MHz, C₆D₆): δ 25.67 (s). Anal. Calcd for C₃₂H₆₁N₄OsP₂Rh: C, 40.61; H, 6.51; N, 5.92. Found: C, 40.68; H, 6.86; N, 6.13. T_1 (ms, OsH₃, 300 MHz, toluene- d_8): 172 (290 K); 87 (250 K); 76 (230 K); 116 (210 K); 325, 271 (190 K).

Preparation of OsH₃(Hpz)(pz)(PⁱPr₃)₂ (5). A suspension of OsH₂-Cl₂(PⁱPr₃)₂ (200 mg, 0.35 mmol) in 18 mL of toluene was first treated with NaBH₄ (133 mg, 3.5 mmol) and then dropwise with 1.8 mL of methanol. After being stirred for 20 min at room temperature, the solution was filtered through Kieselguhr. The filtrate was treated with Hpz (47.66 mg, 0.70 mmol) and heated under reflux for 45 min. The colorless solution was filtered through Kieselguhr and concentrated to ca. 0.5 mL. Addition of methanol caused the precipitation of a white solid, which was decanted, washed twice with methanol, and dried in vacuo: yield 193 mg (85%). IR (Nujol): ν (OsH) 2140 cm⁻¹. ¹H NMR (200 MHz, C₆D₆, 293 K): δ 21.4 (br, 1 H, NH), 7.96, 7.60 and 6.32 (all br, each 2 H, =CH pz), 1.82 (m, 6 H, PCH), 1.02 (dvt, $N = 12.4$ Hz, $J(\text{HH}) = 6.8$ Hz, 36 H, PCCH₃), -11.92 (t, $J(\text{PH}) = 12.5$ Hz, 3 H, OsH). ³¹P{¹H} NMR (80.98 MHz, C₆D₆): δ 22.80 (s, q in off-resonance). Anal. Calcd for C₂₄H₅₂N₄OsP₂: C, 44.42; H, 8.09; N, 8.63. Found: C, 44.54; H, 7.77; N, 8.55. T_1 (ms, OsH₃, 300 MHz, CD₂Cl₂): 270 (293 K), 125 (253 K), 82 (233 K), 74 (213 K), 93 (203 K).

Preparation of [OsH₃(Hpz)₂(PⁱPr₃)₂]BF₄ (6). A solution of **5** (100 mg, 0.15 mmol) in 18 mL of diethyl ether was treated with HBF₄ (8.5 μ L, 0.15 mmol) and stirred at room temperature for 2 h. The resulting white solid was decanted, washed with diethyl ether, and dried in vacuo: yield 99 mg (90%). IR (Nujol): ν (NH) 3220–3480, ν (OsH) 2160, ν (BF₄) 980–1200 cm⁻¹. ¹H NMR (300 MHz, CD₂Cl₂, 293 K): δ 10.72 (br, 2 H, NH), 7.85, 7.80 and 6.45 (all br, each 2 H, =CH pz), 1.98 (m, 6 H, PCH), 0.97 (dvt, $N = 12.8$ Hz, $J(\text{HH}) = 6.9$ Hz, 36 H, PCCH₃), -12.53 (t, $J(\text{PH}) = 12.4$ Hz, 3 H, OsH). ³¹P{¹H} NMR (121.42 MHz, CD₂Cl₂): δ 24.5 (s, q in off-resonance). Anal. Calcd for BC₂₄F₄H₅₃N₄OsP₂: C, 39.12; H, 7.27; N, 7.61. Found: C, 39.25; H, 7.65; N, 7.82. T_1 (ms, OsH₃, 300 MHz, CD₂Cl₂): 75 (233 K), 67 (213 K), 89 (193 K).

Preparation of OsH₃Cl(Hpz)(PⁱPr₃)₂ (7). Method a. A solution of **5** (75 mg, 0.122 mmol) in 10 mL of toluene was treated with 1 mL (0.122 mmol) 0.12 M of a toluene–HCl solution. After being stirred for 30 min at room temperature, the solution was concentrated to ca. 0.5 mL. Addition of methanol (3 mL) causes the precipitation of a white solid, which was decanted, washed with 2 mL of methanol, and dried in vacuo: yield 30 mg (40%).

Method b. A solution of **6** (100 mg, 0.147 mmol) in 10 mL of THF was treated with NaCl (8.6 mg, 0.147 mmol). After being stirred for 30 min at room temperature, the solution was concentrated to ca. 0.5 mL; addition of methanol (3 mL) caused the precipitation of a white solid, which was decanted, washed with 2 mL of methanol, and dried in vacuo: yield 40 mg (44%). IR (Nujol): ν (NH) 3228, ν (OsH) 2172, 2148 cm⁻¹. ¹H NMR (300 MHz, C₆D₆, 293 K): δ 13.35 (br, 1 H, NH), 7.50, 6.37 and 5.73 (all br, each 1 H, =CH pz), 2.00 (m, 6 H, PCH), 1.16 (dvt, $N = 12.6$ Hz, $J(\text{HH}) = 6.9$ Hz, 18 H, PCCH₃), 0.97 (dvt, $N = 12.0$ Hz, $J(\text{HH}) = 6.6$ Hz, 18 H, PCCH₃), -12.83 (t, $J(\text{PH}) = 12.6$ Hz, 3 H, OsH). ³¹P{¹H} NMR (121.42 MHz, C₆D₆): δ 23.76 (s, q in off-resonance). Anal. Calcd for C₂₁ClH₄₉N₂OsP₂: C, 40.80; H, 8.00; N, 4.53. Found: C, 40.55; H, 7.80; N, 4.62. T_1 (ms, OsH₃, 300 MHz, toluene- d_8): 290 (293 K); 140 (253 K); 103 (233 K); 71 (213 K); 91, 112 (193 K).

X-Ray Structure Analysis of (PⁱPr₃)₂H₃Os(μ -biim)IrCOD (4). Crystals suitable for single X-ray crystal analysis were obtained by slow diffusion of methanol into a concentrated solution of **4** in acetone. A summary of crystal and refinement data is reported in Table 3. The prismatic crystal studied was glued on a glass fiber and mounted on a

Table 3. Crystal Data and Data Refinement for (PⁱPr₃)₂H₃Os(μ -biim)IrCOD (**4**)

formula	C ₃₂ H ₆₁ IrN ₄ OsP ₂	Z	2
fw	946.228	λ , Å	0.610 73
space group	P1̄ (No. 2)	ρ (calcd), g cm ⁻³	1.784
a, Å	8.978(2)	Z	2
b, Å	13.629(3)	μ , mm ⁻¹	7.49
c, Å	15.369(3)	R ^a	0.0237
α , deg	79.34(2)	R _w ^b	0.0274
β , deg	86.31(2)	S ^c	1.314
γ , deg	72.43(1)		

^a $R = \sum|[F_o - F_c]|/\sum F_o$. ^b $R_w = \sum(w^{1/2}|F_o - F_c|)/(\sum w^{1/2}F_o)$. ^c $S = \{\sum(w|[F_o - F_c]|^2)/(M - N)\}^{1/2}$, where M is the number of observed reflections and N is the number of data.

Siemens AED-2 diffractometer. Cell constants were obtained from the least-squares fit of the setting angles of 50 reflections in the range $20 \leq 2\theta \leq 48^\circ$. The 11 279 recorded reflections were corrected for Lorentz and polarization effects. Three orientation and intensity standards were monitored every 55 min of measuring time; no variation was observed. Reflections were also corrected for absorption by an empirical method.³⁷

The structure was solved by Patterson (Ir and Os atoms) and conventional Fourier techniques. Refinement was carried out by full-matrix least-squares with all non-hydrogen atoms anisotropic. The hydrido ligands were clearly located and treated as free isotropic atoms in a full-matrix least-squares refinement using the SHELXTL-PLUS program. The values of $\sigma[d(\text{H}-\text{H})]$ were calculated from the atomic coordinates and their estimated standard deviations, including the calculated cell errors, and checked by the PARST93 and PLATON programs. Although the estimated standard deviations obtained are certainly low, it should be pointed out that these values are similar to those found in related structures of polyhydrides determined by X-ray crystallography, where similar specific experimental and refinement conditions were applied (low temperature, high-angle data collection, high-ratio reflections/parameters, completely free isotropic atoms).^{3f,38} Remaining hydrogens were located from difference Fourier maps or fixed in idealized positions (C–H = 0.96 Å) and included in the refinement riding on carbon atoms with common isotropic thermal parameters. Atomic scattering factors, corrected for anomalous dispersion for Ir, Os, and P, were taken from ref 39. The function minimized was $\sum w([F_o] - [F_c])^2$ with the weight defined as $w = 1/(\sigma^2[F_o] + 0.000372[F_o]^2)$. Final R and R_w values were 0.0237 and 0.0274. All calculations were performed by use of the SHELXTL-PLUS system of computer programs.⁴⁰

Acknowledgment. We thank the DGICYT (Project PB 92–0092, Programa de Promoción General del Conocimiento) and EU (Project: Selective Processes and Catalysis Involving Small Molecules) for financial support. E.O. thanks the Diputación General de Aragón (DGA) for a grant.

Supporting Information Available: Tables of atomic coordinates, anisotropic thermal parameters, experimental details of the X-ray study, bond distances and angles, and interatomic distances for **4** (9 pages). An X-ray crystallographic file in CIF is available for (PⁱPr₃)₂H₃Os(μ -biim)IrCOD on the Internet. Access and ordering information is given on any current masthead page.

IC960446+

(37) Walker, N.; Stuart, D. *Acta Crystallogr.* **1983**, A39, 1581.

(38) (a) Leeaphon M.; Fanwick, P. E.; Walton, R. A. *Inorg. Chem.* **1991**, 30, 4986. (b) Maltby P. A.; Schlaf, M.; Steinbeck, M.; Lough, A. J.; Morris, R. H.; Klooster, W. T.; Koetzle, T. F.; Srivastava, R. C. *J. Am. Chem. Soc.* **1996**, 118, 5396.

(39) *International Tables for X-Ray Crystallography*; Kynoch Press: Birmingham, England, 1974; Vol. IV.

(40) Sheldrick, G. M. *SHELXTL PLUS*; Siemens Analytical X-Ray Instruments, Inc.: Madison, WI, 1990.